Open Access

Check for updates

Research Article

Journal of Veterinary and Animal Sciences
ISSN (Print): 0971-0701, (Online): 2582-0605
https://doi.org/10.51966/jvas.2025.56.4.558-565

Collagen coated HASi granules as a substitute for artificial periosteum for the repair of critical size femoral defects in rat models#*

Navya P. Shibu[1] , P.T. Dinesh[1*], B.F. Francis[2], M.K. Narayanan[3], S. Sooryadas[1], N.S Jinesh[1] Kumar, V. Remya[1], M. Pradeep[4] and Hamza Palekkodan[4]

[1]Department of Veterinary Surgery and Radiology, [4]Department of Veterinary Pathology, College of Veterinary and Animal Sciences, Pookode, Wayanad – 673 576, [2]BMT Wing, SCTIMST, Trivandrum, [3] Department of Veterinary Surgery and Radiology, College of Veterinary and Animal Sciences, Mannuthy, Thrissur - 680651, Kerala Veterinary and Animal Sciences University, Pookode, Wayanada, Kerala, India

Citation: Shibu, P.N., Dinesh, P.T., Francis, B.F., Narayanan, M.K., Sooryadas, S., Kumar, N.S.J., Remya, V., Pradeep, M. and Palekkodan, H.2025 Collagen coated HASi granules as a substitute for artificial periosteum for the repair of critical size femoral defects in rat models. *J. Vet. Anim. Sci.* **56** (4): 558-565

Received: 09.06.2025 Accepted: 25.10.2025 Published: 31.12.2025

Abstract

This study evaluated the regenerative potential of a mineralised collagenous periosteum in critical-size femoral defects in rats. A six-millimetre diaphyseal defect was created in the right femur of all animals and was grafted with a hydroxyapatite (HA)-doped collagen sleeve filled with silica-coated hydroxyapatite (HASi) granules. Healing was assessed using radiography, histology and bone turnover markers. The test graft showed early integration with host bone by the fourth week, evidenced by cortical bridging and medullary recanalisation by week twelve. Radiographically, the test graft material remained stable throughout the healing process and achieved complete healing by week twelve, while bone turnover marker analysis confirmed the early initiation of bone regeneration. Histological examination revealed uniform new bone deposition and advanced bone maturation with well-organised lamellar bone and bone marrow by week twelve, without signs of inflammation or fibrous tissue proliferation. The study demonstrated the bone healing efficacy of HA-doped collagen sleeve filled with HASi granules in critical-sized femoral defects in rats.

Keywords: *Periosteum, collagen sleeve, HASi, bone grafting*

Comminuted fractures, removal of bone tumours and cysts can create segmental defects in the diaphysis of bones, often resulting in significant functional impairment and morbidity in animals. Conventional treatments for these conditions can lead to bone shortening, delayed healing or non-union. Though the periosteum plays a crucial role in bone healing, its availability is limited in cases of extensive bone damage (Goldberg and Akhavan, 2005). The most effective approach involves substituting the lost bone segment with either natural bone or synthetic materials. However, due to the drawbacks of autografts and allografts, researchers are focused on developing materials that closely mimic natural bone using tissue engineering and biotechnology. Bioengineered periosteum is designed to replicate the structure and function of natural periosteum, making it a promising candidate for promoting bone regeneration (Li *et al.,* 2016). A key innovation in this area is the use of collagen-coated HASi granules in the fabrication of artificial periosteum. This combination offers multiple benefits, including providing a natural scaffold for cell attachment, proliferation and differentiation. Additionally,

**Corresponding author: dineshpt@kvasu.ac.in, Ph. 9447144085*

HASi granules enhance mechanical stability and improve the integration of the graft material with the surrounding tissue (Zhengwei *et al.,* 2021). Before being incorporated to clinical practice, this material requires a comprehensive evaluation in animal models. Therefore, the present study was undertaken with the following objective of evaluating the regeneration potential of mineralised collagenous periosteum and triphasic silica coated hydroxyapatite composite bioceramic (HASi) in critical size femoral defects in the rat model.

Materials and methods

The study was conducted in accordance with the guidelines set by the Committee for Control and Supervision of Experiments on Animals (CCSEA) and was approved by the Institutional Animal Ethics Committee of the College of Veterinary and Animal Sciences, Pookode, Kerala Veterinary and Animal Sciences University (IAEC/COVAS/PKD/22/2/2024). Fifteen adult male Wistar rats, aged 16 weeks with an average body weight of 300 grams were randomly selected for the study. The animals were housed under controlled conditions with natural light cycles and were fed ad-libitum with standard rat mash and clean drinking water. Feed was withdrawn one hour before anaesthesia, while water was provided until the time of anaesthesia.

The right thigh of each animal was shaved, cleaned, degreased with 70 per cent alcohol and disinfected with povidone-iodine solution. Rats were premedicated with 0.05 mg/kg of buprenorphine hydrochloride subcutaneously 20 minutes before anaesthesia. Anaesthesia was induced with intraperitoneal injections of xylazine hydrochloride and ketamine hydrochloride at 3 mg/kg and 30 mg/kg, respectively. Anaesthesia was maintained with 1–2 per cent isoflurane in 100 per cent oxygen and the animals were placed in left lateral recumbency.

A linear incision was made from the greater trochanter (proximal landmark) to the femoro-tibio-patellar joint (distal landmark). A white line corresponding to the intermuscular septum between the biceps femoris and superficial gluteal muscles was identified (Fig. 1) and the muscles were bluntly separated with Metzenbaum scissors to expose the femur (Costa *et al.*, 2011). A six-millimetre full-thickness diaphyseal segmental defect was created using a suitable bur (Fig. 2). The defect was bridged with the HA-doped collagen sleeve consisting of type I collagen reinforced with hydroxyapatite ($Ca_{10}(PO_4)_6(OH)_2$) and filled with HASi granules composed of hydroxyapatite and silica (SiO_2), providing a bioactive, bone-mimicking composite (test material) donated by Bioceramics Laboratory, Biomedical Technology Wing (BMT), Sree Chitra Tirunal Institute for Medical Sciences and Technology, Trivandrum (SCTIMST). The graft material and bone fragments were secured using 1.5 mm five-hole microplates and 1.5 mm x 6 mm cortical screws (Fig. 3).

Postoperatively, the animals were administered ceftriaxone sodium at 40 mg/kg intramuscularly twice daily for seven days. Analgesia was achieved with buprenorphine at 0.05 mg/kg subcutaneously once a day for three days and meloxicam at 2.0 mg/kg subcutaneously for five days. The skin wound was dressed with povidone-iodine ointment twice daily and the sutures were removed on the 10th postoperative day. Three rats were periodically sacrificed by administering an overdose of thiopentone sodium (5 per cent) intraperitoneally at 2, 4, 8 and 12 weeks of post-grafting to collect samples for evaluating the healing process.

Immediate postoperative radiographs were taken to assess the fracture reduction and graft material positioning. Orthogonal radiographic views were taken under light anaesthesia to monitor the healing process at the 2nd, 4th, 8th and 12th weeks postoperatively. The radiography settings used were 45 kV and 9.5 mAs at a focal distance of 100 cm**.** Radiographic scoring was done based on the presence or absence of fracture line, integration of graft materials and remodelling. Three radiographs each at different stages of healing were given to six persons who were unaware of the stage of healing and scored. The observers were divided into two groups in which three were novice and three were experienced persons in assessing the radiographic healing (Dinesh, 2018). The scores ranged from 0 to 10 where “0” denotes “No- healing” and “10” denotes “Complete healing”. The criteria included neo-osteogenesis, proximal and distal graft to host-bone integration and bone remodelling.

Fig. 1. Approach to femur

Fig. 2. After creating critical sized defect

Fig. 3. After completing grafting procedure

The fractured femur was harvested periodically during 2nd, 4th, 8th and 12th weeks postoperatively and the thickness of the diaphysis at the site of fracture was compared to that of the contralateral bone in each animal.

Blood was collected from the retro-orbital venous plexus under anaesthesia. Serum samples were used to estimate serum alkaline phosphatase and acid phosphatase activity at different time points postoperatively.

Three rats each were sacrificed at regular intervals during 2nd, 4th, 8th and 12th weeks postoperatively to evaluate healing through histological examination. The implantation site, along with normal bone was harvested and fixed in 10 per cent neutral buffered formalin. Bone pieces were decalcified, sectioned and stained using routine haematoxylin and eosin (H&E) stain. Representative sections from each sample were subjected to Masson's Trichrome staining to demonstrate new bone formation.

Histomorphometric analysis was performed on H&E-stained sections, evaluating parameters such as inflammation, vascularity and new bone formation using a semiquantitative grading system described by Qiu *et al.* (2007).

Results and discussion

Male Wistar rats were chosen for this experiment due to their availability, ease of handling and robustness. Male rats were preferred over females, following Mills and Simpson (2012) who observed that the reproductive cycles of females can influence bone healing. Rodents being small and manageable are ideal for biomaterial research in orthopedics as noted by Li *et al.* (2015). Yang *et al.* (2024) pointed out that the cylindrical shape of the femur allows for more stable osteosynthesis and improved soft tissue coverage compared to other long bones.

Diagnostic imaging

All animals tolerated the treatment protocol well and the surgical incisions healed without any complications. Immediate postoperative radiographs of animals showed effective reduction of fracture fragments and correct placement of the graft material. A radiolucent line was observed both proximally and distally at the graft-host interface on the immediate postoperative radiograph (Fig. 4). According to Dinesh (2018), the presence of this line suggested that integration between the host bone and graft had not occurred. By the second week, the graft material exhibited increased density compared to previous radiographs likely due to cellular ingrowth through the graft's pores. This enhanced radiopacity indicated progressive fracture healing and highlighted the osteoconductive and osteo-integrative properties of the graft material (Dinesh *et al.,* 2018; Rao *et al.,* 2021; Manasa, 2023). Radiolucency was noted only at the distal graft-host interface, suggesting early integration of the graft material with the host bone at the proximal end. Rao *et al.* (2021) and Manasa (2023) also employed the same parameter, opining that the absence of a radiolucent line indicated successful integration between the graft and host bone (Fig. 5). By fourth week, the graft material was fully integrated with the host bone at both interfaces, with no radiolucent zone between the graft and distal fragment (Fig. 6). This finding was consistent with the findings of Dinesh *et al*. (2018), who observed complete integration of HASi bio-ceramic grafts by that time. Parizi *et al.* (2012) reported similar findings in their study, where critical ulnar defects in rabbits were treated with corals and human platelet-rich plasma.

By eight weeks, radiographic integration between the graft and host bone was complete, and the graft showed reduced radiographic density (Fig. 7). Additionally, partial canalisation of the medullary cavity was observed. These findings aligned with reports from Nair (2009) and Suresh *et al.* (2017) who noted a decrease in graft density as a sign of osteogenesis and material degradation.

By twelve weeks, complete radiographic healing was observed as indicated by cortical bridging and

Fig. 4. Immediate post-operative radiograph with visible radiolucent line and proximal and distal interface

Fig. 5. At 2nd week: Radiolucent line visible at distal bone-graft interface

Fig. 6. At 4th week: radiolucent line barely visible at bone-graft interface of distal region

Fig. 7. At 8th week: Complete absence of radiolucent line at host bone and graft interface

Fig. 8. At 12th week: Cortical bridging and medullary recanalis-ation

Table 1. Radiographic healing scores

Radiographic healing scores					
Stage of healing	Bone formation	Proximal union	Distal union	Remodelling	Total score
2nd Week	1.00±0.26	0.56±0.16	0.89±0.28	0.56±0.16	3.01±0.11
4th Week	2.22±0.31	1.77±0.14	1.78±0.14	1.11±0.10	6.88±0.22
8th Week	3.87±0.44	1.89±0.29	0.89±0.29	1.22±0.14	7.87±0.66
12th Week	3.96±0.55	2.00±0.23	2.00±0.23	1.87±0.26	9.83±0.50

Table 2. Gross morphology at the healed site

Time Interval	Diameter of shaft at the defect site (Mean ± SE) in cm		Proximal Integration	Distal Integration
	Left	Right		
2nd Week	0.32±0.02	0.33±0.02	Present	Absent
4th Week	0.33±0.02	0.35±0.00	Present	Present
8th Week	0.35±0.03	0.63±0.01	Present	Present
12th Week	0.35±0.00	0.65±0.02	Present	Present

medullary recanalisation. The radiographic density of the graft material had significantly reduced and was barely visible (Fig 8). Dinesh (2018) investigated the efficacy of HASi bioceramics for treating critical-sized femoral defects in rats and found that the defects had healed and fully integrated with the surrounding host bone by the 12th week postoperatively. Comparable results were also noted by Manasa (2023).

Radiographs taken during different phases of healing were given to six persons who were unaware of the stage of healing. The scores ranged from 0 to 10 where "0" denoted "No- healing" and "10" denoted "Complete healing". The criteria used were formation of bone, union of proximal and distal fragments with grafts and remodelling. The results of the present study indicated good progressive integration of the graft material with the host bone and thereby healing (Table 1). Material degradation equivalent with the formation of new bone was also noticed radiographically. Similar observations were noted by Nair *et al.* (2011), Dinesh *et al.* (2018) and Rao *et al.* (2021) in their studies conducted in goat and rat femoral segmental defect models treated with HASi.

Gross morphology of implantation site

Gross morphological changes at the implanted site were evaluated at 2nd, 4th, 8th and 12th weeks postoperatively by examining the bones collected from humanely sacrificed animals. At 2nd week, union between the graft and host bone was observed at the proximal interface. By 4th week, complete integration of graft material with both proximal and distal interfaces was evident. This might be due to the differences in biological and mechanical conditions like richer blood supply and higher metabolic activity, providing more nutrients and oxygen for bone regeneration. The thickness of the femur shaft at the defect site was measured at the time of sacrifice using a Vernier caliper and compared with the thickness of the opposite femur (Table. 2).

Table 3. Serum biochemical parameters

Day of surgery	Serum alkaline phosphatase activity (IU/L)	Serum acid phosphatase activity (IU/L)
Day 0	127.38 ± 7.20	2.47 ± 0.49
2nd week	165.09 ± 3.57	4.53 ± 0.31
4th week	155.20 ± 3.43	3.36 ± 0.18
8th week	148.03 ± 15.61	4.12 ± 1.10
12th week	122.59 ± 2.60	3.63 ± 0.14

Serum biochemical parameters

Bone turnover markers including serum ACP and serum ALP activity were estimated on the day of surgery and at weeks 2, 4, 8 and 12, postoperatively (Table. 3).

The mean serum alkaline phosphatase (ALP) activity increased to 165.09 ± 3.57 IU/L from the preoperative value of 127.38 ± 7.2 IU/L. Since alkaline phosphatase is considered as a marker for bone formation, this increase could be attributed to early initiation of the bone healing process by two weeks itself. Similar findings were also reported by Dinesh (2018) and Manasa (2023), where the initial increase in ALP values was attributed to osteoblastic activity occurring during fracture repair. At 4th week, ALP levels remained elevated at 155.20 ± 3.43 IU/L, showing no significant change compared to preoperative values. According to Dinesh (2018), alkaline phosphatase was a phosphate splitting enzyme produced actively by osteoblasts in large quantity that was released into the osteoid matrix to initiate the deposition of minerals during fracture repair. This value corresponded to the ongoing reparative process of the bone. By the 8th week, ALP activity started to decline but was still elevated at 148.03 IU/L. A similar observation was reported by Manasa (2023), where ALP activity showed a gradual decrease from the 4th to the

8th week. This result contrasted with the findings of Dinesh (2018) and Anu (2023), who reported elevated ALP values during 8th week postoperatively. By the 12th week, ALP levels returned to near-normal values at 122.59 ± 2.6 IU/L, indicating the completion of the healing process. Similar variations in ALP were also noted by Dinesh (2018) and Anu (2023).

The mean serum acid phosphatase activity was 2.47 ± 0.49 IU/L on the day of surgery. The values increased to 4.53 ± 0.31 IU/L by the second week and 3.36 ± 0.18 IU/L by the fourth week. In the eighth and twelfth weeks, a gradual decrease was observed, with average values of 4.12 ± 1.1 IU/L and 3.63 ± 0.14 IU/L, respectively which indicated the completion of healing process. These observations were not comparable with the results of Manasa (2022) where the acid phosphatase activity reduced gradually from day of surgery to 12th week postoperatively and Anu (2023) where ACP value increased by week 8th and 12th postoperatively.

Histological evaluation

The grafted site and host bone were harvested at 2, 4, 8 and 12 weeks post-surgery and tissue sections were prepared following decalcification. These sections were stained with H&E and Masson's Trichrome to evaluate the cellular response during the healing process.

By second week, the defect was primarily composed of fibrous tissue with high level of vascularity with healing initiating from edges of periosteum of host bone and advancing toward the centre of defect. Periosteal activation and the presence of hypertrophic chondrocytes were evident towards the defect edge without any signs of inflammation. Defect site displayed areas of osteoblasts characterised by deposition of more organised collagen around them, which was evident from Masons trichrome staining (Fig: 9). By 4th week, the amount of woven bone increased at defect site by replacing fibrosis tissue. Edge bone integration along with the overall healing score had improved significantly as compared from 2nd week.

On 8th week, defect site exhibited a mixture of woven and lamellar bone with moderate level of edge bone integration at both the proximal and distal ends of the defect accompanied by mild vascularisation, fibrosis and without any infiltration of mononuclear cells. On 12th week, bone healing was almost complete with the

2nd Week

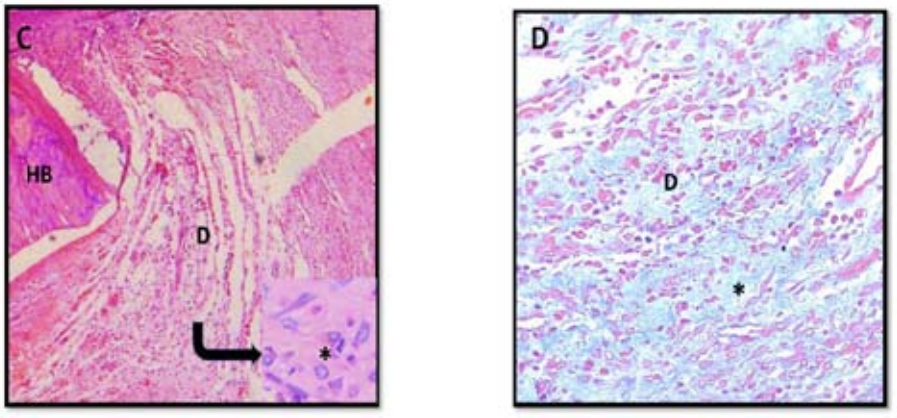

Fig. 9. C. Fibrous tissue and osteoblastic proliferation (*) in defect (x40, H & E). **D.** Well organised collagen deposition (* blue colour) in defect site (x400, Mason's Trichrome). D- defect site, HB- host bone.

4th week

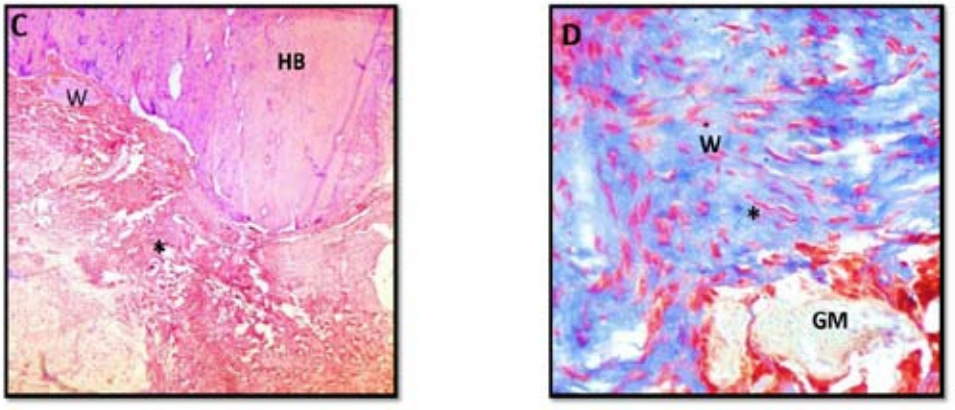

Fig. 10. C. Scattered islands of woven bone (W) and newly synthesised osteoid matrix (*) in defect site (x40, H and E). **D.** Sheet of woven bone (* blue colour) filling the defect area (x400, Mason's Trichrome). HB- host bone, D- defect.

8th week

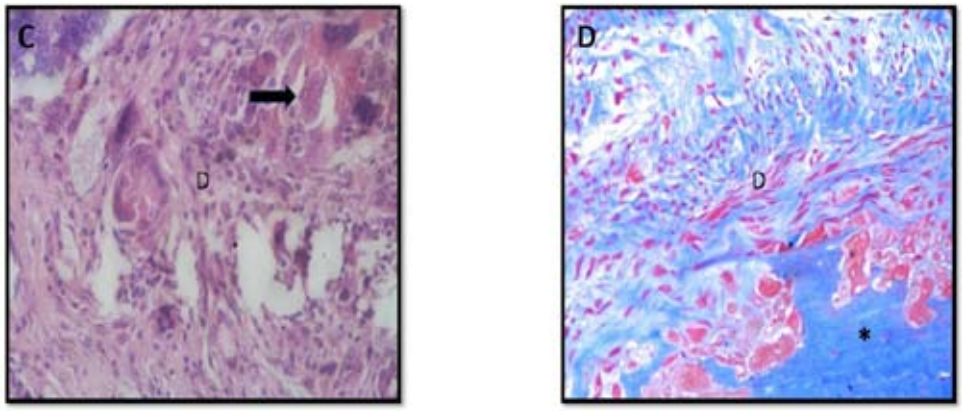

Fig. 11. C. Defect filled by sheets of woven bone and developing Harversian system (arrow) (x400, H & E). **D.** Lamellar (* bright blue colour) and woven bone (light blue colour) at defect site (x400, Mason's Trichrome). D- Defect.

12th week

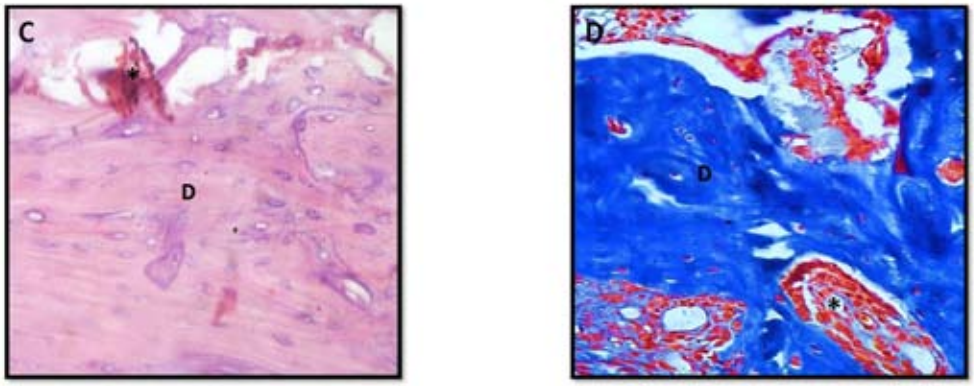

Fig.12. C. Diffused zone of lamellar bone at defect site with bone marrow formation (*) (x400, H & E). **D.** Lamellar bone (bright blue colour) with bone marrow at defect site (* red colour) (x400, Mason's Trichrome). D-defect**.**

presence of lamellar bone with osteocytes arranged around Harversian system in treatment group. The total healing score also increased significantly in both groups with extensive levels of edge bone integration without any sign of inflammation. Similar observations are made by Peng *et al.* (2023), where the volume and compactness of mature trabecular and lamellar bone appeared to be more in treatment containing mineralised collagen membrane.

HASi exhibits several characteristics that make it highly effective for bone regeneration. Its interconnected porous structure facilitates cellular infiltration, nutrient transport and vascularisation, while hydroxyapatite ensures excellent biocompatibility and supports osteogenic cell adhesion. The inclusion of silica enhances the material's bioactivity by promoting osteoblast differentiation and encouraging the formation of bone-like apatite. Its controlled degradation rate maintains mechanical stability while allowing gradual replacement by natural bone tissue. Collectively, these features accelerate bone repair, enhance mineral deposition and improve integration with surrounding tissue highlighting HASi as a promising scaffold for repairing critical-sized bone defects.

Histomorphometric analysis was performed by counting various cell types in six randomly chosen fields from both the proximal and distal interfaces of the defect on each slide. Each parameter including the degree of inflammation, neovascularisation, fibrosis, new bone type, new bone quantity and edge bone integration was scored accordingly (Table 4).

Table 4. Histomorphometric scoring

Histomorphometric scoring							
Time interval	Inflammation	Vascularity	Fibrosis	New bone type	New bone amount	Edge bone integration	Total score
2nd week	3.00± 0.00	2.58± 0.28	1.50± 0.31	1.08± 0.08	1.50± 0.15	0.83± 0.24	10.4 ±1.28
4th week	3.00± 0.00	2.50± 0.23	2.50± 0.13	1.25± 0.13	1.83± 0.11	1.75± 0.24	12.83±0.26
8th week	3.00± 0.00	1.83± 0.38	3.00± 0.00	1.75± 0.21	2.25± 0.17	2.00± 0.25	13.83±0.23
12th week	3.00± 0.00	2.75± 0.25	3.00± 0.00	3.00± 0.00	2.33± 0.25	2.41± 0.14	16.49±0.12

Conclusion

On summarising the findings from the present research work, it could be inferred that critical size segmental defects could be successfully corrected with the use of HA doped collagen sleeve filled with HASi granules. The porous nature of HASi had helped in faster bone repair and mineralised collagen sleeve had effectively promoted the osteogenic differentiation of MSCs, inhibited macrophage proliferation, fusion and reduced fibrous capsule formation, resulting in faster bone regeneration.

The collagen-coated HASi cylinder and collagen sleeve performed effectively in promoting bone regeneration, though a few limitations were noted. Minor variations in porosity and mechanical strength occasionally affected consistency between samples. The bonding between the HASi cylinder and collagen sleeve could be further improved for better structural integrity. Additionally, since the study was conducted in rat models, further evaluation in larger animal models is needed to confirm clinical applicability.

Further investigations are needed to overcome the existing limitations and enhance the overall performance of the material. Upcoming research should focus on refining the fabrication techniques to achieve greater uniformity and mechanical stability. Extended *in vivo* and biomechanical assessments are essential to validate the long-term functionality of the regenerated bone. Incorporation of bioactive agents or growth factors could further promote osteogenesis and angiogenesis. Moreover, testing in larger animal models will be crucial to evaluate the translational and clinical potential of this composite scaffold in bone tissue engineering.

Acknowledgements

The authors gratefully acknowledge the Dean, College of Veterinary and Animal Sciences, Pookode, Kerala Veterinary and Animal Sciences University for providing the necessary facilities and support for the successful conduct of this study. We also extend our sincere thanks to the faculty members of the Department of Veterinary Surgery and Radiology and Veterinary Pathology for their valuable guidance, encouragement and assistance throughout the course of the work.

Conflict of interest

The authors declare that they have no conflict of interest

References

Costa, C.M., Bernardes, G., Ely, J.B. and Porto, L.M. 2011. Proposal for access to the femur in rats. *Int. J. Biotechnol*. **2:** 73-79.

Anu D, Fernandez, F.B., Parathazhathayil, D., Surendran, S., Mampilly, P., Sainulabdeen, A., Remya, V. and Harikrishna, V. 2024. Effects of polyvinyl alcohol–hydroxyapatite composite ceramic on calvarial defects with critical size in rat models. *Lab. Anim. Res.* **3**: .40-46.

Dinesh, P. T. 2018. Healing of bone defects treated with tri-phasic composite bio- ceramic in rat models. *Ph.D. thesis*. Kerala Veterinary and Animal Sciences University, Pookode, 142p.

Dinesh, P.T., Venugopalan, S.K., Martin, J.K.D., Devanand C.B., Pillai, U.N. and Nair, D. 2018. Radiographic evaluation of healing of critical size defects of femur treated with tri-phasic composite bio- ceramic implants in rat models. *Indian J. Nat. Sci.* **9**: 15504-15507.

Goldberg, V. M. and Akhavan, S. 2005. In: Friedlaender, G.E. and Lieberman, J.R. (ed.), *Bone Regeneration and Repair: Biology and Clinical Applications*. (1st Ed.). Springer, New York, pp. 57-65.

Li, N., Song, J., Zhu, G., Li, X., Liu, L. and Shi, X. 2016. Periosteum tissue engineering-A review. *Biomater. Sci.* **4:** 1554–1561.

Li, Y., Chen, S., Li, L., Qin, L., Wang, X. and Lai, Y. 2015. Bone defect animal models for testing efficacy of bone substitute biomaterials. *J. Orthop. Translation.* **3**: 95-104.

Manasa, M., Dinesh, P.T., Fernandez, F.B., Sooryadas, S., Palekkodan, H., Anoop, S., Jineshkumar, N.S., Remya, V. and Varma, H.K. 2023. Radiographic evaluation of healing of critical size calvarial defects treated with decellularised tissue engineered HASi in rat models. *J. Vet. Anim. Sci.*, **54**: 916-920.

Mills, L. and Simpson, A. 2012. *In vivo* models for bone repair. *J. Bone Jt. Surg.* **94**: 865-874.

Nair, M.B., Varma, H.K. and John, A. 2009. Triphasic ceramic coated hydroxyapatite as a niche for goat stem cell-derived osteoblasts for boneregeneration and repair. *J. Matr. Sci. Matr. Med.* **20:** 251-258.

Parizi. A.M., Oryan, A., Sarvestani, S.Z. and Bigham, A.S. 2012. Human platelet rich plasma plus Persian Gulf coral effects on experimental bone healing in rabbit model: radiological, histological, macroscopical and biomechanical evaluation. *J. Mater. Sci. Mater Med.* **23:** 473-483.

Peng, F., Zhang, X., Wang, Y., Zhao, R., Cao, Z., Chen, S., Ruan, Y., Wu, J., Song, T., Qiu, Z. and Yang, X. 2023. Guided bone regeneration in long-bone defect with

a bilayer mineralized collagen membrane. *Collagen and Leather*. **5:** 36.

Qiu, Q.Q., Mendenhall, H.V., Garlick, D.S. and Connor, J. 2007. Evaluation of bone regeneration at critical-sized calvarial defect by DBM/AM composite. *J. Biome. Matr. Res. Appl. Biomater.* **81:** 516-523.

Rao, R., Dinesh, P.T., Sooryadas, S., Chandy, G. and Mathew, M. 2021. Successful utilization of triphasic silica containing ceramic coated hydroxyapatite (HASi) for the treatment of comminuted tibial fracture in a goat: a case report. *J. Vet. Anim. Sci*. **52:** 200-203.

Suresh, D., Syam, K.V., Chandy, G., Sooryadas, S. and Deepa, P.M. 2017. Radiographical evaluation of Sr-HASi bioceramic substitute for critical size bone defect in a goat- Clinical study. *J. Vet. Anim. Sci*. **48**: 40-42.

Yang, Q., Xu, M., Fang, H., Gao, Y., Zhu, D., Wang, J. and Chen, Y. 2024. Targeting micromotion for mimicking natural bone healing by using NIPAM/Nb2C hydrogel. *Bioact. Mater*. **39:** 41-58.

Zhengwei, Li., Du, T., Ruan, C. and Niu, X. 2021. Bioinspired mineralised collagen scaffolds for bone tissue engineering. *Bioact. Mater*. **6:** 1491- 1511. ■